ECOLOGY

Soil warming increases the number of growing bacterial taxa but not their growth rates

Dennis Metze[1,2]*, Jörg Schnecker[1], Coline Le Noir de Carlan[3], Biplabi Bhattarai[4], Erik Verbruggen[3], Ivika Ostonen[4], Ivan A. Janssens[3], Bjarni D. Sigurdsson[5], Bela Hausmann[6,7], Christina Kaiser[1], Andreas Richter[1,8]*

Copyright © 2024 The Authors, some rights reserved; exclusive licensee American Association for the Advancement of Science. No claim to original U.S. Government Works. Distributed under a Creative Commons Attribution NonCommercial License 4.0 (CC BY-NC).

Soil microorganisms control the fate of soil organic carbon. Warming may accelerate their activities putting large carbon stocks at risk of decomposition. Existing knowledge about microbial responses to warming is based on community-level measurements, leaving the underlying mechanisms unexplored and hindering predictions. In a long-term soil warming experiment in a Subarctic grassland, we investigated how active populations of bacteria and archaea responded to elevated soil temperatures (+6°C) and the influence of plant roots, by measuring taxon-specific growth rates using quantitative stable isotope probing and ^{18}O water vapor equilibration. Contrary to prior assumptions, increased community growth was associated with a greater number of active bacterial taxa rather than generally faster-growing populations. We also found that root presence enhanced bacterial growth at ambient temperatures but not at elevated temperatures, indicating a shift in plant-microbe interactions. Our results, thus, reveal a mechanism of how soil bacteria respond to warming that cannot be inferred from community-level measurements.

INTRODUCTION

One major challenge in climate change research is understanding its effects on the soil microbiome, which is crucial for global climate projections (*1*–*3*). Soil microorganisms are important climate regulators, governing carbon fluxes an order of magnitude larger than anthropogenic CO_2 emissions (*4*, *5*). Accelerated microbial activities due to warming might increase soil carbon losses and thereby exacerbate climate change. Carbon stocks in high-latitude soils are particularly vulnerable to microbial decomposition because the microbes inhabiting them are often temperature-limited and tend to be more responsive to warming (*6*, *7*). Whether a soil microorganism becomes more active with warming depends on the complex interplay of many factors such as its genetic makeup, substrate availability (*8*, *9*), or its interactions with plants and predators. Although accounting for microbial responses is important for improving predictions of soil carbon dynamics (*3*), many aspects remain elusive. Specifically, we lack an understanding of the physiological response of individual microbial taxa to warming and have major knowledge gaps on how warming affects plant-microbe interactions (*1*, *2*, *10*–*13*).

Growth is the central component of a microorganism's physiology and is closely linked to soil carbon fluxes (*14*–*16*). Growth is restricted to the active part of the soil microbial community. Despite constituting only a few percent of the total community (*17*), the active microbial community is the main driver of soil carbon and nutrient cycling (*11*, *17*, *18*). Recent estimates suggest that growing microorganisms in soil account for >95% of the respiration of the entire community with growing cells being 1000 times more active than starved ones (*19*). Rising temperatures have a large impact on the physiological processes of soil microbes including their growth rates and, therefore, soil carbon fluxes.

Microbial growth in warmed soils has been predominantly measured at the total community level, aggregating over thousands of different populations. Growth responses to warming (measured as relative community growth; mass-specific growth) range from positive (*9*, *20*), over neutral (*9*) to negative (*20*, *21*) with seasonal variation. Short-term warming often accelerates microbial process rates. Over time, however, many of these rates tend to return to their initial state that is thought to be mediated by community shifts, substrate loss, or physiological acclimation (*22*–*24*). In a (Sub)Arctic grassland, which is also subject of this study, long-term warming has caused notable losses of soil carbon and nitrogen, resulting in a reduction of microbial biomass (*8*). While this did not affect microbial growth and respiration rates per unit of soil mass, rates of relative community growth and respiration per unit of microbial biomass (mass-specific) increased with temperature and stayed elevated even after more than 50 years of warming. This was interpreted as a persistent acceleration of microbial activities without signs of thermal acclimation (*8*). In this system, warming caused a down-regulation of the microbial protein biosynthesis machinery that possibly freed energy available for accelerated activity (*25*). However, warming was also found to increase maintenance and respiratory costs (*25*, *26*).

Community-aggregated measurements of growth and respiration are useful to indicate directions of warming responses. Nonetheless, they integrate more than thousands of microbial populations with varying growth and carbon use characteristics (*27*), which hampers their capacity to detect underlying microbial mechanisms. Detecting these mechanisms is crucial to comprehend the dynamic processes that underlie microbial warming responses and is needed to improve their prediction. Quantitative stable isotope probing (qSIP) using ^{18}O water can hereby be a powerful tool because it allows estimating

[1]Centre for Microbiology and Environmental Systems Science, University of Vienna, Vienna, Austria. [2]Doctoral School in Microbiology and Environmental Science, University of Vienna, Vienna, Austria. [3]Research Group Plants and Ecosystems, University of Antwerp, Antwerp, Belgium. [4]Department of Geography, Institute of Ecology and Earth Sciences, University of Tartu, Tartu, Estonia. [5]Faculty of Environmental and Forest Sciences, Agricultural University of Iceland, Hvanneyri, Borgarnes, Iceland. [6]Joint Microbiome Facility of the Medical University of Vienna and the University of Vienna, Vienna, Austria. [7]Division of Clinical Microbiology, Department of Laboratory Medicine, Medical University of Vienna, Vienna, Austria. [8]International Institute for Applied Systems Analysis, Advancing Systems Analysis Program, Laxenburg, Austria.
*Corresponding author. Email: dennis.metze@univie.ac.at (D.M.); andreas.richter@univie.ac.at (A.R.)

Downloaded from https://www.science.org on June 23, 2025

growth rates of individual microbial populations based on the incorporation of ^{18}O into microbial DNA (*28*). qSIP can be used to quantify the growth response of distinct microbial taxa to warming from which shifts in ecosystem-scale rates ultimately emerge. A recent improvement of this technique, vapor-SIP, allows us to label soil water without the addition of liquid water and, thus, enables us to estimate taxon-resolved microbial growth near in situ conditions (*29*).

Plants are another important factor affecting and controlling microbial activities by providing primary carbon resources through litter production and root exudates. Soil microorganisms that live in association with roots consume plant-derived carbon and show higher potential growth rates (*30*, *31*). Climate change alters plant performance, including litter and exudate production and litter quality, with potential repercussions for the soil microbiome and the carbon cycle (*32*). For instance, warming can increase plant productivity, causing greater carbon allocation belowground and promoting microbial activities (*33*). On the other hand, warming can compromise plant performance, reducing rhizodeposition or inducing plant-microbe competition, for instance, when nitrogen is limiting (*34*). The effects of soil warming on roots seem to differ between ecosystems. While warming has been reported to increase either fine root production or fine root biomass in a boreal peatland (*35*) and a mountainous forest (*36*), it has been found to reduce both in (Sub) Arctic grasslands (*37*, *38*). Fine root biomass is particularly important for root-associated taxa because it determines the root surface where exudates are released. Warming might also affect root exudate quality and seasonality if it causes shifts in the plant community structure. Overall, indirect warming effects mediated by plants can have a strong impact on soil microorganisms. In some cases, these effects might be stronger than direct warming effects, especially if microbes are adapted to live in association with roots. However, it remains elusive how climate change shapes the direction of plant-microbe interactions (*2*, *12*, *13*).

To better understand the microbial warming response and more accurately predict microbial activities in a future climate, we need to look beyond community-aggregated growth estimates and acknowledge that these activities emerge from a diverse set of active populations, shaped by direct and indirect warming effects. Studying them accordingly will allow us to scrutinize interpretations derived from community-aggregated measurements and might lead to deeper insights into how soil microbes respond to warming.

Here, we investigated the impact of more than 50 years of natural geothermal soil warming on the growing populations of bacteria and archaea in a (Sub)Arctic grassland in Iceland. We also examined how their responses were shaped by indirect warming effects mediated by roots. We used water vapor equilibration ^{18}O-qSIP (vapor-qSIP) to identify growing (hereafter, also, active) taxa of bacteria and archaea in soil and quantify their growth rates at ambient and elevated soil temperatures (+6°C). Root-ingrowth (1 mm mesh) and root-exclusion (30 μm mesh) cores were used to elucidate the impact of plants on microbial growth. We installed these cores in the field for 10 months and extracted them at peak vegetation season, along with an undisturbed soil core. Using these three soil core types, we aimed to disentangle direct and indirect warming effects. We had three primary objectives. First, we aimed to decipher the growth patterns of individual bacterial and archaeal populations following long-term warming and compare them to community-level estimates. Second, we aimed to investigate how the presence of roots affected their growth patterns and whether plant-microbe interactions changed under long-term warmed conditions, particularly considering previously reported decreases in fine root biomass and production. Third, we aimed to examine whether taxa of the same genus or family showed similar growth responses to warming and root presence, possibly elucidating group-specific traits.

RESULTS

Soil carbon and nitrogen are lost with long-term warming while relative community growth increases

We took three different soil cores (undisturbed, root ingrowth, and root exclusion) across four replicated temperature gradients in a long-term warmed (Sub)Arctic grassland (fig. S1) to differentiate between direct warming effects (undisturbed) and indirect warming effects mediated by roots (root ingrowth and root exclusion) on soil biogeochemical and microbial parameters (Fig. 1A). Long-term warming (+6°C) altered soil carbon and nitrogen pools, soil water content, relative community growth rates, and extracellular enzyme activities. Long-term warming reduced the concentrations of soil carbon (Fig. 1B) and soil nitrogen (table S1; $t = 2.56$, df = 21.9, $P = 0.017$) by 18 and 19%, respectively, and decreased volumetric water content from 41 ± 3% (means ± SD) to 36 ± 4% ($t = 3.35$, df = 21.8, $P = 0.0028$). Warming and root presence increased exoglucanase (Warming: $F = 8.8$, $P = 0.01$; $Core_{root\ presence/absence}$: $F = 5.7$, $P = 0.033$) and exochitinase activities (Warming: $F = 21.5$, $P < 0.001$; $Core_{root\ presence/absence}$: $F = 4.6$, $P = 0.05$) but did not affect phosphatase and protease activities. Measurements of more dynamic pools such as dissolved organic carbon and total dissolved nitrogen did not differ between cores and warming levels (table S1). In addition, microbial biomass carbon and total 16*S* ribosomal RNA (rRNA) gene copy numbers did not significantly differ between warmed and control plots. However, relative community growth rates increased with warming (Fig. 1C), similar to previous reports. These microbial community growth rates were determined on the basis of the ^{18}O enrichment of the unfractionated DNA and, thus, inherently also included other microorganisms such as fungi. When averaging relative community growth across cores for each warming level, we found it to rise by 53% with long-term warming of 6°C.

Root effects on community composition are only captured when differentiating between active and inactive taxa

After 10 months of field incubations, the absence of roots did not affect total community composition estimated via amplicon sequencing. However, roots affected which members of the total community were active and growing. To compare the composition of total and growing communities of bacteria and archaea, we performed a principal components analysis (PCA) using Euclidean distances based on amplicon sequence variant (ASV) absolute abundances (16*S* rRNA gene copies per ASV, centered log-transformed). Hereafter, the term "bacteria" is used to encompass both bacteria and archaea for brevity.

Long-term warming caused significant shifts in the composition of the total communities and rendered them more variable compared to ambient conditions (Fig. 2A). Root presence, however, did not affect the composition of the total communities. This changed when subsetting total communities for their growing taxa. We found growing communities to be distinct in each treatment with roots and warming having significant effects on their composition (Fig. 2B). In contrast to the total communities, core type [= root presence; coefficient of determination (R^2) = 0.26] and its interaction with warming

Downloaded from https://www.science.org on June 23, 2025

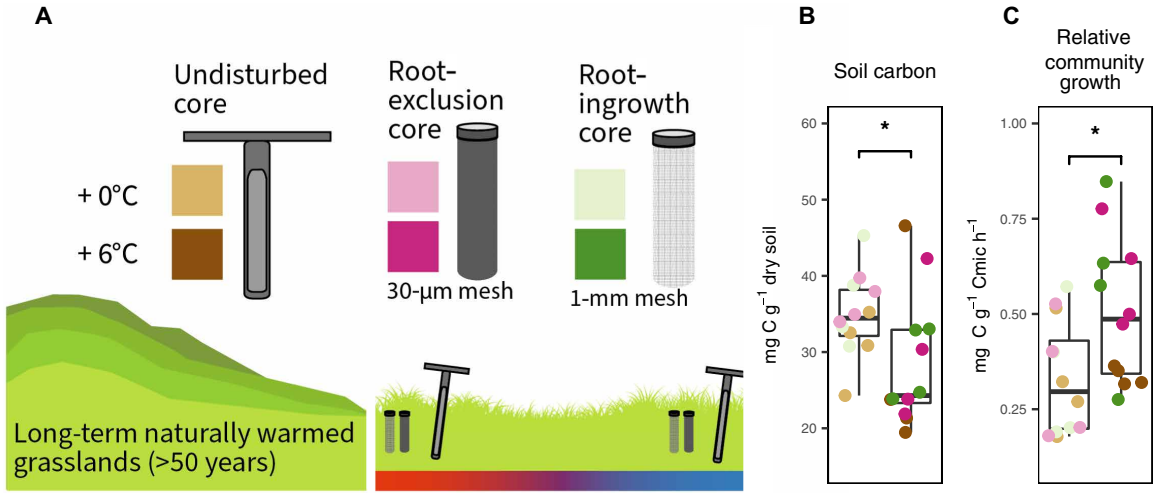

Fig. 1. Experimental design, soil carbon, and relative microbial community growth. (**A**) Soil samples were taken from four replicated temperature gradients ($n = 4$ biological replicates) in a (Sub)Arctic grassland in Iceland. This grassland experienced at least 50 years of soil warming established by natural geothermal activity. Root-ingrowth and root-exclusion cores were installed in situ for 10 months (October 2019 to August 2020) at two temperature levels (ambient temperatures and +6°C above ambient temperatures). We aimed to investigate how root presence or absence affects microbial growth under warmed conditions. While extracting the in situ installed cores, we also took a fresh soil core (hereafter, undisturbed core) to examine warming effects without the disturbances associated with core installation (e.g., soil extraction, mixing, and root/stone removal). Squares depict treatment colors used for graphs. (**B**) Concentrations of soil carbon decreased with warming ($t = 2.1$, df = 18.3, $^*P = 0.049$, $n = 12$), while (**C**) relative microbial community growth (mass-specific) increased ($t = -2.5$, df = 20.7, $^*P = 0.019$, $n = 12$). The median is represented by the center line of the box, while the upper and lower quartiles are indicated by the box limits. The whiskers represent 1.5 times the interquartile range; any outliers are shown as separate points. We used two-sided Student's *t* tests to infer differences between warming levels.

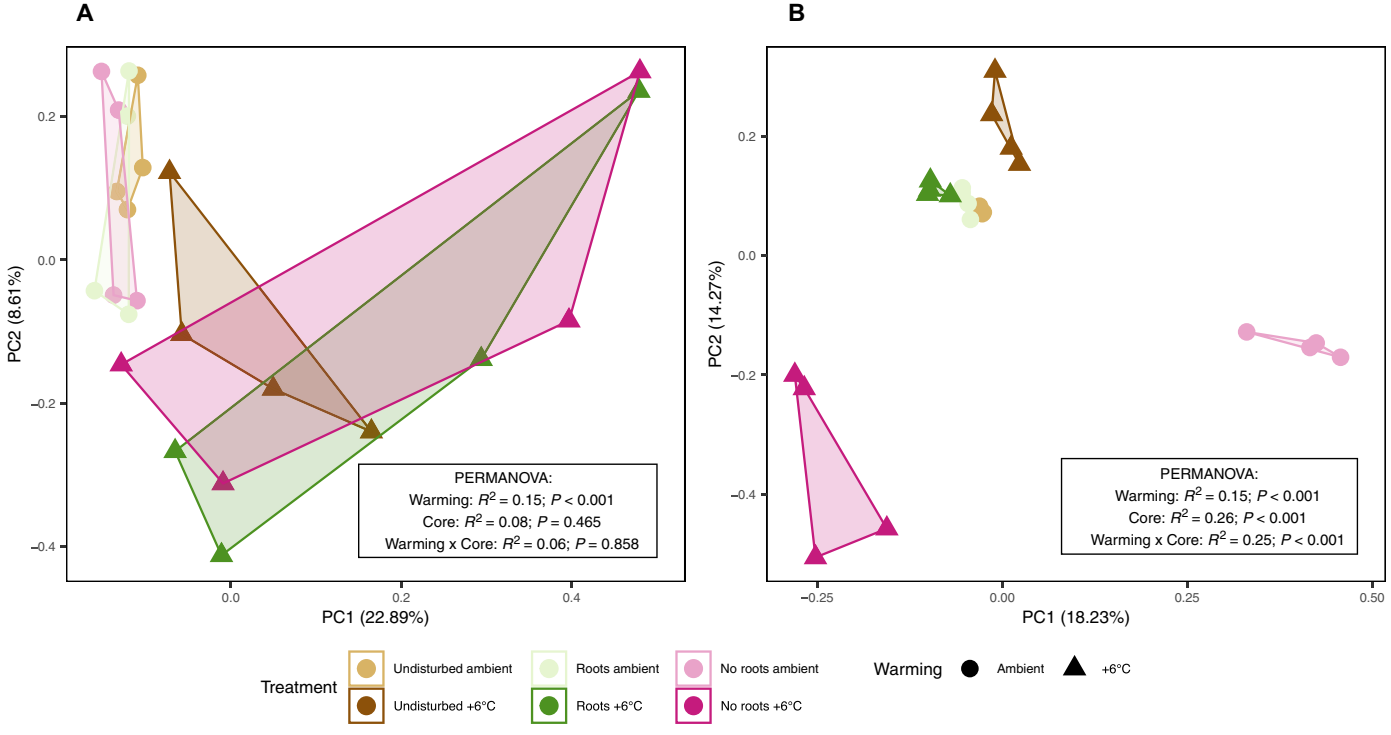

Fig. 2. Root effects are only captured when examining growing communities. PCA of total (**A**) and growing (**B**) bacterial and archaeal communities from fresh undisturbed soil cores (brown), root-ingrowth cores (mesh size, 1 mm, green), and root-exclusion cores (mesh size, 30 µm, pink). PCA was performed using Euclidean distances on the basis of centered log ratio–transformed ASV absolute abundances [digital droplet PCR (ddPCR) inferred 16*S* rRNA gene copies multiplied by amplicon sequencing reads]. Absolute abundances were aggregated over the density fractions of each sample gradient. Statistics from two-way permutation-based multivariate analysis of variance (PERMANOVA; $n = 4$ biological replicates) are provided as inset panels (factors: $\text{Warming}_{\text{ambient/+6°C}}$ and $\text{Core}_{\text{undisturbed/root ingrowth/root exclusion}}$). PC, principal component.

Downloaded from https://www.science.org on June 23, 2025

($R^2 = 0.25$) had a greater impact on the composition of the growing communities than warming alone ($R^2 = 0.15$). The composition of the growing communities that formed in the absence of roots was particularly different from those cores where roots were present (undisturbed cores and root-ingrowth cores). Overall, this highlights that analyses only based on amplicon sequencing data without additional growth information were not able to capture root effects.

Long-term warming does not increase average bacterial growth rates but causes twice as many taxa to become active

To describe the general effects of long-term warming, we focused on samples from the undisturbed cores because they were not exposed to any disturbances connected to core installation. The number of growing taxa, their contribution to the total community, and their relative growth rates (RGRs) served as indicators for microbial shifts in response to long-term warming. The number of growing ASVs (Fig. 3A) almost doubled with warming (ambient, 342 ± 32 ASVs; warmed, 797 ± 115 ASVs; means ± SD), also increasing the percentage of the total community that was growing (Fig. 3B) from on average 1.6 to 4.6%. The increase in the number of growing taxa was reflected across most major phyla but differed in extent (Fig. 3D). While Actinobacteriota, Bacteroidota, and Chloroflexi harbored twice as many growing taxa under long-term warming, there were almost three times as many Acidobacteriota and Proteobacteria. We found that many of these shifts were driven by specific families (fig. S2). For instance, the Xanthobacteraceae, a family of the Proteobacteria, showed a more than eight times higher richness of growing taxa at elevated temperatures (fig. S2). The Xanthobacteraceae was also responsible for a significantly larger proportion of community growth at higher temperatures (fig. S3).

Despite higher microbial community growth (Fig. 1C), long-term warming did not accelerate average taxon-specific growth rates (Fig. 3C), so bacterial populations were generally not growing faster. This was supported by directly comparing RGRs of ASVs active at both temperatures that did not increase either (fig. S4B). If we included nongrowing taxa [atom percent excess (APE) $^{18}O = 0$] in these calculations, then average taxon-specific growth increased slightly but not significantly (fig. S4A). At the level of the whole bacterial community, we observed that the total and relative growth approximately doubled at higher temperatures (fig. S5, A and B). Although this increase was only significant for the relative growth ($P = 0.042$), these bacterial community patterns corresponded to the rise in microbial community growth (Fig. 1C) and the increase in the richness of growing bacterial taxa (Fig. 3A). Community growth correlated with the number of growing bacterial taxa (fig. S6). This held for the whole microbial community ($R^2 = 0.13$, $P = 0.082$; fig. S6A) and the bacterial community ($R^2 = 0.81$, $P > 0.001$; fig. S6A), albeit only significant for the latter. In addition, taxa that became only active with elevated temperatures did not grow faster than populations exclusively active in ambient soils (fig. S7B).

Different bacterial taxa become dominant with long-term warming

Although average growth rates did not increase, individual taxa showed clear responses to warming. Because the contribution of soil microorganisms to biogeochemical processes is not only connected to their growth rates but also their abundance, we integrated both by calculating proportional ^{18}O assimilation rates. Proportional ^{18}O assimilation (range, 0 to 1) is a relative value, expressing how much a single ASV contributes to the total growth of the active community. Hence, it can also be considered as the proportion of bacterial growth an ASV is responsible for.

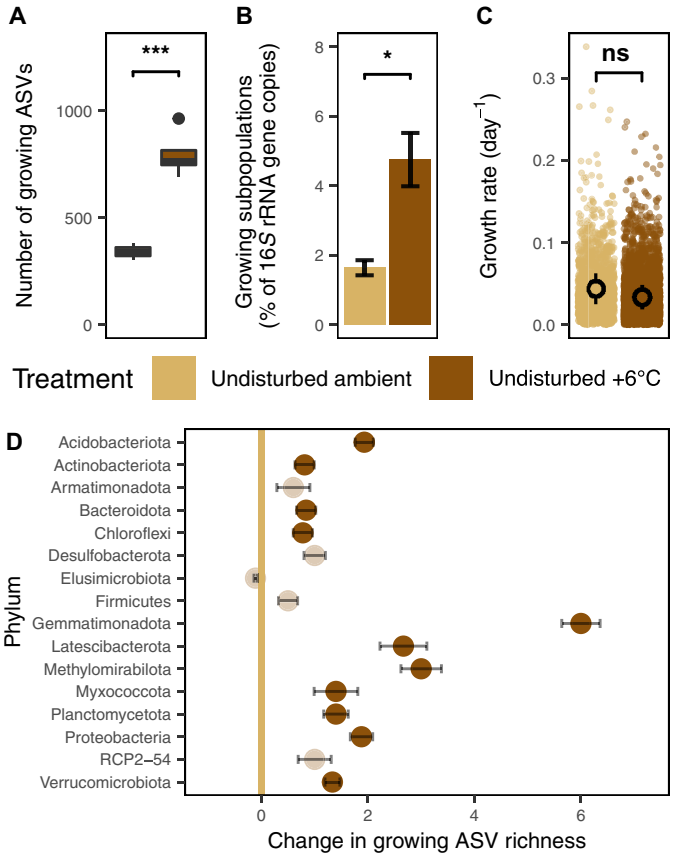

Fig. 3. Warming increases the richness of growing taxa and their share of the total community but not their mean growth rates. Number of unique growing ASVs (**A**), their proportion of the total community expressed as the share of 16*S* rRNA gene copies (**B**), mean taxon-level growth rates (**C**), and warming-induced relative changes in the number of growing taxa within major phyla (**D**). Light-colored dots in (C) represent ASV-level growth rates from all replicates used to calculate means ($n = 4$ biological replicates) and SEs (points, error bars). Points in (D) represent relative changes (0 = no change and 1 = increase by 100%) in the number of growing taxa per phylum including SEs. Bold colored points denote significant shifts (Kruskal-Wallis test and false detection rate correction for multiple comparisons, $n = 4$) and transparent points nonsignificant (ns) ones. The vertical line depicts the mean of the reference treatment (undistributed core at ambient conditions) used to calculate relative changes. Asterisks [(A) ***$P > 0.001$, (B) *$P = 0.04$] represent significant differences ($n = 4$) inferred by two-way ANOVA (factors: $\text{Warming}_{\text{ambient/+6°C}}$ and $\text{Core}_{\text{undisturbed/root ingrowth/root exclusion}}$) followed by Tukey post hoc tests.

At ambient temperatures, the top 20 ASVs based on their proportional ^{18}O assimilation accounted for 36 to 46% of the community growth (Fig. 4A). Most of these taxa lost their dominant role with long-term warming where they were only responsible for 3 to 11% of the community growth. Dominant growing taxa at ambient temperatures belonged to the genera *Collimonas*, *Flavisolibacter*, *Granulicella*, *Kitatospora*, *Pseudomonas*, *Puia*, *Streptoacidiphilus*, *Terracidiphilus*, and *Undibacterium*, showing a high proportion of Bacteroidota. Three ASVs remained among the top ^{18}O assimilators (*Collimonas* ASV 2,

Downloaded from https://www.science.org on June 23, 2025

Fig. 4. Different taxa become dominant contributors to the total community's growth with long-term warming in undisturbed cores. Heatmap showing taxa (ASVs) with the highest proportional ^{18}O assimilation in undisturbed cores at ambient (**A**) and warmed (**B**) conditions, visualized across individual samples (boxes, $n = 4$ biological replicates). Proportional ^{18}O assimilation is calculated using recomputed relative abundances of only growing taxa (sum: relative abundances$_{growing\ taxa} = 1$) and their RGRs; it represents the contribution of an ASV to the total community's growth. Hence, it can also be considered as the proportion of bacterial growth an ASV is responsible for. ASVs were ranked on the basis their proportional ^{18}O assimilation per replicate. After retaining the top 15 ASVs across all replicates per treatment (total$_{ambient}$, 33 ASVs; total$_{warmed}$, 39 ASVs), we visualized the top 20 ASVs using heatmaps. (A) Top taxa at ambient temperatures; (B) Top taxa under warming. Bubbles below each replicate show the cumulative growth summarized over all displayed ASVs. ASVs were only considered if they were growing in at least two samples per treatment. If genus or family identity could not be assigned (NA), then phylum names were provided.

Kitatospora ASV 5, and *Streptoacidiphilus* ASV 10) even after long-term warming (bold ASV names, Fig. 4B). Their contribution to the total community's growth was lower though and less consistent across replicates. Many top assimilatory taxa at elevated temperatures were uncharacterized members of the Acidobacteriota, which lacked taxonomic assignment at the order level. Other ASVs belonged to the genera *Bradyrhizobium*, *Mucilaginibacter*, *Puia*, and the unclassified Acidobacteriota RB41. At higher temperatures, community growth was more evenly distributed among a larger number of taxa. The top 20 ASVs accounted for less community growth than at ambient conditions with only 15 to 41%. Under long-term warming, community growth generally comprised fewer dominant taxa, indicating a larger evenness across active taxa. For instance, more than twice as many taxa were required to account for 50% of the community growth in warmed plots [59 ± 25 ASVs (means ± SD); fig. S8] than at ambient temperatures (26 ± 5 ASVs).

Long-term warming alters root effects on bacterial growth

To disentangle how roots affect the growth of soil bacteria and archaea today and in a warmer climate, we installed root-ingrowth and root-exclusion cores in situ for 10 months. At ambient conditions, root presence accelerated growth rates on average ~2.3 times as compared to root-exclusion cores [Fig. 5A; two-way analysis of variance (ANOVA); Warming: $F = 2.4$, $df = 1$, $P = 0.138$; Core: $F = 8.85$, $df = 2$, $P = 0.002$; Warming x Core: $F = 10.98$, $df = 2$, $P = 0.0007$]. In long-term warmed soils, however, this effect was lost (Fig. 5A). Warming significantly decreased RGRs in root inclusion cores, so they were indistinguishable from those estimated from root-exclusion cores (Fig. 5A). Most growing taxa were exclusively active in one specific core type, indicating a closer association with either roots or bulk soil (fig. S9). We defined putative root–associated and bulk-soil–associated taxa as those exclusively growing in either the presence or absence of roots. We found that root-associated were growing faster than bulk-soil–associated taxa at ambient temperatures, whereas this effect was not significant for shared taxa growing in both cores (fig. S7A). The two functional groups also differed in their warming response. Putative root–associated taxa showed a negative growth response to warming (fig. S7B) indicated by a decrease in mean growth rates (Fig. 5B). Putative bulk-soil–associated taxa responded to long-term warming in an opposite manner. Their mean growth rates either increased with warming (Fig. 5C) or remained constant (fig. S7B).

Downloaded from https://www.science.org on June 23, 2025

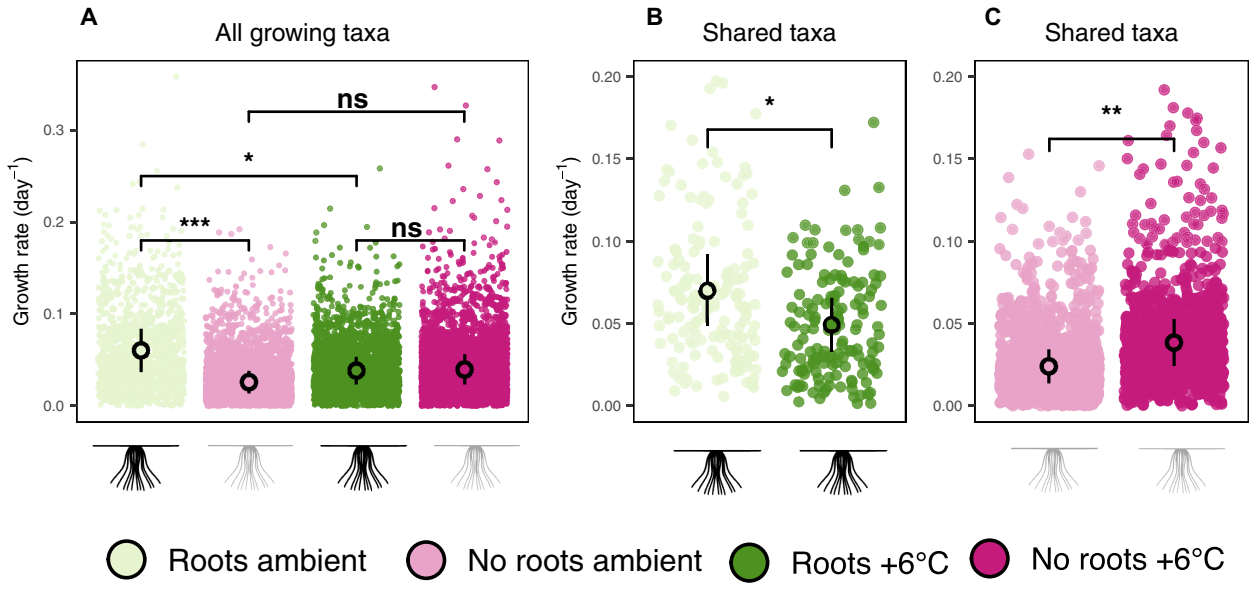

Fig. 5. Warming alters the effect of roots on bacterial and archaeal growth rates. Mean taxon-level RGRs of all taxa growing in root-ingrowth and root-exclusion cores at ambient and warmed conditions (**A**). Mean taxon-level RGRs of shared growing taxa between ambient and warmed conditions in root-ingrowth (**B**; Student's *t* test: $t = 2.8$, df = 4.05, $^{*}P = 0.046$) and root-exclusion (**C**; Student's *t* test: $t = -4.9$, df = 5.41, $^{**}P = 0.003$) cores. Light-colored dots represent ASV-level growth rates across all replicates used to calculate means ($n = 4$ biological replicates) and SEs (points, error bars). Asterisks represent significant differences ($n = 4$) inferred from two-way ANOVA (factors: $\text{Warming}_{\text{ambient/+6°C}}$ and $\text{Core}_{\text{undisturbed/root ingrowth/root exclusion}}$) followed by Tukey post hoc tests [(A) $^{*}P = 0.022$, $^{***}P > 0.001$) or inferred from Student's *t* test [(B) and (C)].

At ambient conditions, the richness of growing taxa in root-ingrowth cores was comparable to undisturbed cores (302 ± 106 ASVs; fig. S7) but lower than in root-exclusion cores (968 ± 88 ASVs). Root-ingrowth cores responded to long-term warming with larger and more diverse growing communities, supporting our findings from the undisturbed cores (fig. S10, A and B). In contrast, the diversity and size of growing communities in root-exclusion cores remained unchanged.

Members of the Chitinophagaceae profit from root presence

The growth of several taxa was influenced by the presence or absence of roots. On the basis of their proportional ^{18}O assimilation, we observed specific ASVs from different genera to be linked with the presence roots such as *Alkanindiges*, *Mucilaginibacter*, *Puia,* and *Cytophaga* (fig. S11A). However, most of these taxa stopped growing at higher temperatures. Other taxa showed larger contributions to the community's growth when roots were absent such as unclassified members of the Acidobacteriota, Micropepsaceae, and Xanthobacteraceae (fig. S11B). Few root-specific patterns could be observed at the family level (Fig. 6). We found that the top ^{18}O-assimilating families accounted for similar amounts of community growth across both core types and warming levels, ranging between 42 and 72%. Only Chitinophagaceae and Streptomycetaceae members seemed to consistently profit from the presence of roots with significantly higher proportional growth as compared to root-exclusion cores (Fig. 6). In contrast, proportional ^{18}O assimilation of the Nitrosomonadaceae was larger in root-exclusion cores. Overall, although root association patterns were evident at the ASV level, they were not consistent at the family level, except for Chitinophagaceae and Streptomycetaceae.

DISCUSSION

High-latitude soils contain large carbon stocks that are vulnerable to being lost with warming due to accelerated microbial activities. Our understanding of the underlying mechanisms remains inadequate though, partly because microbial responses to climate change are often measured at an aggregated level, summing over the complexity of an entire community. Here, we disentangled the growth response of individual populations of active bacteria and archaea (hereafter, summarized as bacteria) to more than 50 years of long-term soil warming (+6°C), also accounting for indirect warming effects mediated by roots. Our study demonstrates that accelerated community growth with warming is driven by a strong increase in the number of growing taxa, rather than by an increase in average bacterial growth rates, providing a different mechanistic explanation for the microbial warming response than inferred by community-aggregated measurements. We also show that root presence accelerates bacterial growth rates at ambient conditions, whereas this growth-promoting root effect is lost with long-term warming. Warming even seemed to decrease the growth rates of putative root–associated taxa. This indicates that, for some microbial groups, indirect warming effects may be stronger than direct ones, depending on their life history strategy.

In the (Sub)Arctic, long-term warming has been shown to persistently increase relative microbial community growth and respiration (*8*). This was explained by a permanent acceleration of microbial activities with no signs of thermal acclimation, defined as the return of microbial activities toward pre-warmed rates. We also observed higher microbial community growth rates (including fungi) in long-term warmed soils. For archaea and bacteria, however, the increase in community growth was not associated with generally faster-growing populations. This contrasts the idea that warming just accelerates the

Downloaded from https://www.science.org on June 23, 2025

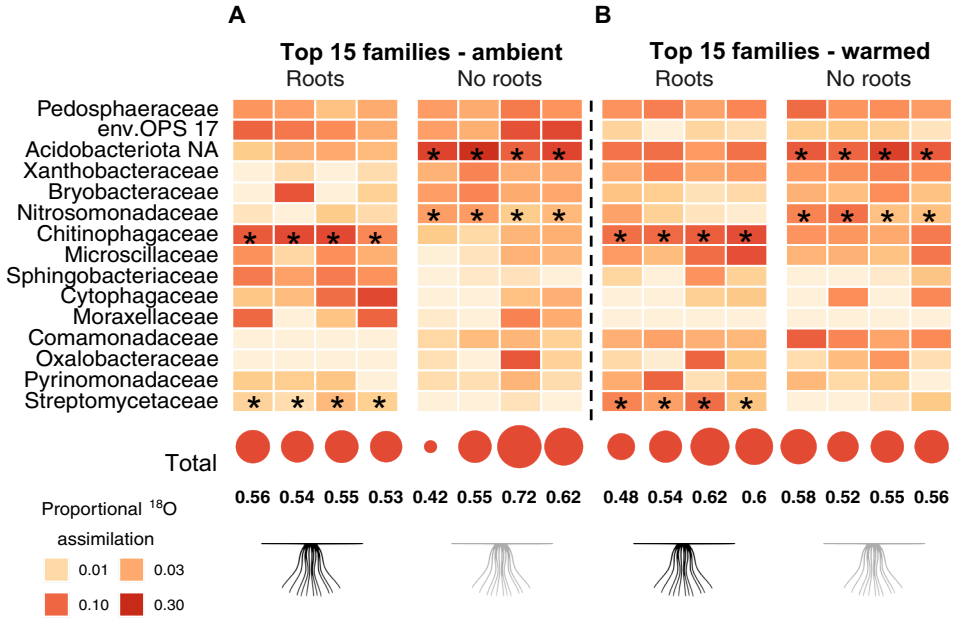

Fig. 6. Chitinophagaceae show a higher contribution to the total community's growth in the presence of roots. Heatmap showing the top 15 families based on their proportional ^{18}O assimilation across root-ingrowth and root-exclusion cores at ambient (**A**) and long-term warmed conditions (**B**). Individual boxes represent replicates per treatment ($n = 4$ biological replicates). Proportional ^{18}O assimilation ranges from 0 to 1 and estimates how much a single taxon contributes to the community's overall growth. Hence, it can also be considered as the proportion of bacterial growth an ASV is responsible for. It was calculated using recomputed relative abundances of only growing taxa (sum: relative abundances$_{growing\ taxa} = 1$) and their RGRs. ASVs had to be active in at least two samples if detected as growing in a treatment. Proportional ^{18}O assimilation was then agglomerated at the family level and visualized for the top 15 families. If family identity could not be assigned (NA), then phylum names were provided. Bubbles below each replicate box show the cumulative growth summarized over all displayed families. Asterisks "*" (Acidobacteriota NA: $P = 0.002$,Nitrosomonadaceae: $P = 0.044$, Chitinophagaceae: $P = 0.004$, Streptomycetaceae: $P = 0.016$) represent significant differences between root-ingrowth and root-exclusion cores agglomerated over both temperature regimes based on Wilcoxon rank tests using false detection rate correction for multiple comparisons ($n = 4$).

growth rates of already present populations (Fig. 3C). Instead, the higher bacterial community growth (fig. S5, A and B) in warmed soils was driven by a doubling of growing taxa (Fig. 3A) as well as a larger proportion of the total community being active (Fig. 3B). While warming led many bacterial taxa to transition from an inactive to an active state, taxa active at higher temperatures were not characterized by higher growth rates. Neither did warming accelerate the growth of taxa active at both temperatures (fig. S4B) or give rise to generally faster-growing bacteria (fig. S7B). Hence, long-term warming did not produce or foster faster-growing bacterial populations but rather caused more cells to enter a state of detectable activity.

Because taxon-specific growth rates were indistinguishable between temperatures, we cannot generally rule out the presence of thermal acclimation at the level of individual populations. Thermal acclimation can be evoked by direct and indirect factors such as physiological acclimation or substrate depletion. Physiological acclimation, possibly due to higher cellular maintenance (*39*) and respiratory costs (*26*), seems likely for those taxa that were shared between warming levels and did not differ in their growth rates. Most taxa, however, showed narrow environmental optima and were growing at either ambient or warmed conditions. Although many additional taxa became active at higher temperatures, they grew at average rates indistinguishable from ambient conditions. This might have been due to indirect factors such as substrate depletion (*8*, *9*) and larger resource acquisition efforts associated with less energy allocated to growth (*40*, *41*). The latter was supported by higher potential extracellular enzyme activities involved in cellulose and chitin degradation in long-term warmed plots, which also points to a reduced availability of substrates. Overall, we could show that increases in bacterial community growth can be driven by a larger number of growing taxa rather than generally faster-growing populations, with the potential for thermal acclimation across several taxa. This highlights that studying individual microbial populations can reveal mechanisms of the soil microbiome's warming response that are masked at the aggregated community level.

Previous reports of higher relative community growth rates in response to long-term warming were inferred by measuring the incorporation of ^{18}O into total microbial DNA (*8*). Hence, these growth measurements encompassed several groups of microorganisms but mostly bacteria, archaea, and fungi. While we observed the same increase in relative community growth (Fig. 1C), we subsequently focused on the contribution of bacteria and archaea and, thus, cannot make assumptions about shifts in fungal growth rates. Our results shed light on the mechanisms of the bacterial warming response to long-term warming, allowing us to disentangle community aggregated measurements. We cannot rule out that fungi responded differently than bacteria and contributed to the rise in microbial community growth with higher growth rates. Our proposed mechanism, therefore, only applies to the bacterial and archaeal part of the microbial community. Nonetheless, we found that microbial community growth also increases with the number of growing bacterial taxa (fig. S6A) which is expected because bacteria and archaea constitute a large part of soil microbial communities.

Downloaded from https://www.science.org on June 23, 2025

Many taxa only became active and started growing at higher temperatures. Warming has been reported to increase soil microbiome diversity based on amplicon sequencing of the 16*S* rRNA gene (*42*–*45*). Optimal growth temperatures of Artic soil microorganisms can range between 23° and 34°C (*46*), which, by far exceeds, regular temperature in high latitude soils. It is possible that the +6°C (ambient, 10.7°C; warmed, 16.7°C) of soil warming studied in our experiment crossed a minimum temperature threshold that enabled many additional taxa to start growing. Warming-induced losses of nitrogen and carbon might have also decreased the competitiveness of taxa adapted to more nutrient-rich environments, as hypothesized for plants, allowing for a larger diversity of active bacteria (*47*). Mean growth rates remained comparable to unwarmed conditions though. Findings from other warming experiments using qSIP underline that local biogeochemical conditions have a strong impact on the microbial response to climate change. While 29 years of warming increased the mean growth of Tundra soil bacteria by more than 150% (*45*), 15 years of warming along an elevational gradient in Arizona reduced the growth of various groups of bacteria by more than 70% (*48*). The diversity of growing taxa in response to warming in these studies either increased or remained unchanged. Similar to our results, field warming in the Antarctic doubled the number of active taxa (*49*). This suggests that shifts in the number of active bacteria may be a fundamental component of the microbial warming response, but the strength of this mechanism might differ between ecosystems.

Plant-microbe interactions play an important role in shaping microbial activities, but how they are affected by warming remains largely unknown. Warming of soil and air can increase plant carbon inputs and promote microbial activities (*50*–*52*). On the other hand, it may also deplete available nutrients such as nitrogen and enhance competition between plants and soil microorganisms (*34*). We found that plants promoted higher growth rates at ambient temperatures, but that this effect was lost with long-term warming, indicating a shift of plant-microbe interactions from positive to neutral (Fig. 5). Root-associated taxa, in particular, showed lower growth rates in warmed plots. This response may be explained by warming-induced losses in fine-root biomass and production, which were reported from our study site (*37*, *38*), also suggesting a reduction in belowground plant carbon allocation (*53*). Root-associated taxa have been found to consume plant-derived carbon and show higher potential growth rates than bulk-soil–associated taxa (*30*, *31*). Because there are indications from the same experimental site that plant carbon inputs did not increase but rather decreased with warming (*37*, *38*), root-associated taxa may have been unable to maintain higher growth rates in warmed plots due to an insufficient supply of extra carbon, likely aggravated by a simultaneous rise in metabolic and respiratory costs (*26*, *39*). Many bulk-soil–associated taxa showed a positive growth response to warming, indicating that their growth was rather limited by temperature than substrate availability. On the other hand, root exclusion could have also reduced competition with root-associated taxa or negative interactions with larger predatory organisms that could not overcome the small mesh size of the root-exclusion cores. Root- and bulk-soil–associated taxa likely differ in their life history traits. Root-associated taxa are adapted to extra carbon provided by plants as indicated by higher potential growth rates and more genes associated with carbon metabolisms (*30*, *31*). Bulk-soil–associated taxa usually do not have access to root exudates and are adapted to a more carbon-limited environment and need to invest more into extracellular enzymes for soil organic matter decomposition. Hence, indirect warming effects driven by shifts in plant-microbe interactions might have had a negligible impact on the growth rates of bulk-soil–associated taxa. Overall, our study provides evidence that in a (Sub)Arctic grassland, the direction of plant-microbe interactions shifts from positive to neutral because of long-term warming. This also suggests that root effects on soil bacteria have become smaller with warming. The strength of the observed root effect differed between microbial groups, possibly due to differences in their life history strategies, because bulk-soil–associated taxa were largely unaffected by shifts in root-microbe interactions.

Do microbial genera or families show similar response patterns to climate change and, if so, could this help us to infer something about their traits? These are well-identified yet open questions in climate change microbiology. We know that growth rates seem to be to conserved across taxonomic groups (*54*). Whether a certain family performs better under warmed conditions remains elusive though. The growth rate of a microorganism is the major component of its fitness (*55*), and, by measuring its change across different environmental conditions, we may infer something about its adaptations and traits. We found that the top 20 taxa, based on their growth and abundance, accounted for >30% of the community growth at ambient temperatures. Most of these taxa lost their dominant role with long-term warming, while other active taxa became dominant contributors to the community's growth, likely better adapted to the conditions at higher temperatures (Fig. 4). Despite strong differences between warmed and control soils at the ASV level, few taxa managed to persist among the top ^{18}O assimilators (*Collimonas*, *Kitasatospora*, and *Streptacidiphilus*) at warmed conditions, suggesting physiological plasticity with regard to temperature. It is worth mentioning that members of these genera show a wide range of defensive properties including the production of various bioactive and antibiotic compounds that might increase their competitiveness at both temperature regimes (*56*–*58*). *Collimonas* is also known to be a fungus-eating genus (*56*).

The same families accounted for very similar proportions of bacterial growth (>60%) at both temperature regimes (fig. S3). Hence, we could not identify any family, except the Xanthobacteraceae, as particularly warming responsive. However, many ASVs and several genera within these families showed a clear warming response. This suggests that the temperature niche of several bacterial families was rather broad, whereas the niche of the individual taxa within these families was considerably smaller.

Root effects were only visible when examining the actively growing community, highlighting the importance of using activity-based techniques such as qSIP to be able to capture indirect warming effects mediated by plants. Despite strong taxon-specific response patterns, which could be used to categorize ASVs into root- and bulk-soil–associated taxa, broad genus- or family-specific trends were scarce. Nevertheless, one family, the Chitinophagaceae, consistently performed better when roots were present, even at both temperature regimes. This indicates that several members of the Chitinophagaceae might be root beneficiaries. Members of this family have been identified from root microbiomes before (*59*–*61*) and potentially protect plants against pathogens such as fungi, harboring enzymes such as chitinases that are involved in fungal cell wall degradation (*62*–*64*). Chitinophagaceae may also decompose cellulose and could have benefited from the root turnover in the root-ingrowth cores (*65*). We detected higher exochitinase and exoglucanase (the latter being involved

Downloaded from https://www.science.org on June 23, 2025

in cellulose degradation) activities in root-ingrowth cores where Chitinophagaceae accounted for a substantial part of the bacterial community growth.

In this study, we demonstrate that more than 50 years of soil warming persistently increased microbial growth at the community level. While this has previously been shown and assumed to be driven by generally faster-growing taxa, we found this response, at least for bacteria, to be caused by a larger body of distinct active taxa, growing at rates indistinguishable from ambient temperatures. This suggests an alternative mechanism behind the warming-induced increase in relative community growth that cannot rule out thermal acclimation at the level of individual bacterial populations. This pattern, i.e., shifts in the number, diversity, and identity of growing taxa, rather than shifts in their individual growth rates might be a central mechanism behind changes in bacterial activity due to environmental change. While there exists supporting evidence from a drought study in a montane grassland (*29*), future studies need to examine whether this is generalizable across ecosystems and disturbances. If yes, then this might add an additional layer of complexity to predicting the microbial warming response, especially in microbial-explicit models. Taxa becoming active under warmed conditions may be functionally different from those active at ambient temperatures including their interactions. If accelerated microbial activities are not driven by the same active community, only working at faster rates, but by a larger active community with a different composition, then a more complex equation may be necessary to model the microbial warming response. Roots also played an important role in shaping bacterial activity, promoting higher growth rates of associated taxa at ambient temperatures, but not anymore after long-term warming. For putative root–associated taxa, indirect warming effects mediated by shifts in root-microbe interactions appeared to be even stronger than direct warming effects. The soil microbiome has often remained a black box regarding its response to climate change, complicating its incorporation into climate models. Our findings shed light on the range of microbial mechanisms underlying the warming response of the soil microbiome, helping to improve our understanding of the fate of soil carbon in a warmer climate.

MATERIALS AND METHODS

Study site, experimental setup, and sample collection

We conducted our study in the frame of the ForHot natural warming experiment located in southern Iceland (64°00'01"N, 21°11'09"W) (*66*). The ForHot experiment consists of naturally warmed grasslands where a soil temperature gradient established due to geothermal activity. Soil temperatures range from ambient conditions (mean annual soil temperature at 10-cm depth, 6.3° ± 0.3°C; means ± SD) to +20°C of warming. The grassland sites differ in their warming history. Soils for this study were sampled from four neighboring fenced transects (fig. S1) located in a long-term warmed valley. The grassland at this site experienced sustained soil warming for >50 years but probably since 1706 (*66*). The distance between ambient and warmed (+6°C) plots was 24.8 ± 7.2 m (means ± SD). Dominant grassland species were *Agrostis capillaris*, *Ranunculus acris*, and *Equisetum pratense* that established over Brown Andosols of approximately pH 5.7 (*8*). The mean annual air temperature and mean annual precipitation recorded at the closest synoptic station were 5.2°C and 1457 mm, respectively.

In October 2019, we installed stainless steel root-ingrowth (mesh size, 1 mm) and root-exclusion (mesh size, 30 μm) cores adjacent to each other along the four temperature gradients that were located next to each other (Fig. 1A). Soil was extracted and transferred into cores (cylindrical meshed compartment; length, 10 cm; diameter, 3.5 cm) in the field after the manual removal of roots and stones. Root-exclusion cores likely also prevented the entry of soil fauna >30 μm, including predators such as larger nematodes and protists, while fungi had unhindered access to both core types. Cores were retracted after 10 months of in situ incubation at peak vegetation season in August 2020. Along with the preinstalled cores, fresh soil samples (undisturbed soil cores) were collected from the top 10 cm in an area adjacent to the permanently monitored warming plots where metal cores were installed (Fig. 1A). These samples were taken to assess the warming effect on the soil microbiome without previous disturbance. For qSIP, we focused on plots along the gradients that experienced on average + 6°C ($n = 4$) of warming and their corresponding controls at ambient temperatures ($n = 4$). Overall, this resulted in 24 samples comprising material from two warming levels and three core types (undisturbed, root ingrowth, and root exclusion). Although warming intensities have been reported stable over time (*66*), they were subject to variation due to fluctuations in geothermal activity. During laboratory incubations, we maintained the previously confirmed temperature difference of +6°C (*8*) between ambient and selected warmed sites. On the basis of temperature measurements from control plots during field sampling, laboratory incubations were performed at 10.7° and 16.7°C, respectively.

Total and microbial carbon and nitrogen pools

Four days after sampling and storage at 4°C, soil was passed through a 2-mm sieve. Soil water content was determined gravimetrically by drying 2 g of fresh soil at 105°C for 24 hours. We analyzed microbial biomass carbon and microbial biomass nitrogen via the chloroform-fumigation extraction method (*67*). One soil subsample (2 g) was chloroform-fumigated for 48 hours before extraction in 15 ml of 1 M KCl solution, whereas another subsample was extracted immediately. After KCl addition, samples were shaken for 30 minutes, filtered through ash-free filters, and stored at −20°C. We analyzed both subsubsets for extractable organic carbon (EOC) and extractable organic nitrogen (EON) on a TOC/N Analyzer (TOC- VCPH/CPNT-NM-1, Shimadzu, Japan). Microbial biomass carbon and nitrogen were then calculated as the difference between fumigated and non-fumigated subsamples using an extraction coefficient of 0.45 (*67*). Total carbon and nitrogen contents were determined from dried, weighed, and finely ground soil aliquots by elemental analyzer–isotope ratio mass spectrometry (EA-IRMS; EA 1110, CE Instruments, Milan, Italy; coupled to a Finnigan MAT Delta Plus IRMS; Thermo Fisher Scientific, Waltham, MA, USA).

Potential extracellular enzyme activities

We measured the potential activities of four extracellular enzymes related to the degradation of cellulose, chitin, proteins, and organic phosphorus using a modified fluorometric method (*68*) (table S2). In short, 50 ml sodium acetate buffer (50 mM, pH 5.8) was added to 1 g of sieved soil and ultrasonicated at approximately 350 J. Fluorogenic methylumbelliferyl (MUF) substrates were used to measure enzymatic cleavage of all enzymes except for protease assays which required an aminomethylcoumarin (AMC) substrate. We prepared one standard row and four analytical replicates for each sample in a black microtiter

Downloaded from https://www.science.org on June 23, 2025

plate by combining 200 µl of mixed sample and 50 µl fluorogenic substrate. Plates were incubated in the dark at room temperature and fluorescence was measured after 10, 60, and 100 min at an excitation wavelength of 365 nm and an emission wavelength of 450 nm (Tecan Infinite M200 fluorimeter, Werfen, Austria). The increase in fluorescence over time was then used to calculate potential enzyme activities.

Quantitative stable isotope probing via ^{18}O water vapor equilibration

Before vapor-qSIP incubations, soil samples were kept at field temperatures for 2 days (10.7° and 16.7°C) to allow microbial communities to acclimate after transportation and storage. Samples for qSIP were incubated with ^{18}O-enriched water and water at natural abundance using the ^{18}O water vapor equilibration method (*69*). In vivo ^{18}O water vapor equilibration avoids changes in soil water content by letting labeled water redistribute into the soil pore space from a spatially separated source in a closed system. By using this method, we could maintain the original moisture of our soil samples while avoiding air-drying and rewetting, potentially masking in situ activities (*69*). Soil samples were sieved to remove rocks, roots, and plant litter. They were weighed in 1.2-ml (~500 mg) cryovials before placing them into 27-ml glass headspace vials. We applied 500 µl of heavy water [97 atomic % (at %)] to the bottom of each headspace vial, which was calculated using the initial soil water content and the target soil water enrichment of ~70 at % ^{18}O. The volumetric water content was 36 ± 4% (means ± SD) in warmed and 41 ± 3% in ambient soils. Headspace vials were closed air-tight with rubber septa after water application and incubated at ambient temperatures and at +6°C above (ambient, 10.7°C; warmed, 16.7°C) for 5 days. To monitor the ^{18}O enrichment of the soil water over time, we prepared an additional ^{18}O-calibration setup for each temperature level using soil samples from one transect. These calibration samples were harvested after 3, 6, and 48 hours to collect the remains of liquid water at the bottom of the headspace vials. At the end of the 5-day incubation period, the same procedure was performed for all other ^{18}O labeled samples. Water samples were analyzed for their ^{18}O enrichment through equilibration of ^{18}O in H_2O with CO_2 by a Gasbench II headspace sampler connected to a Delta V Advantage isotope ratio mass spectrometer (Thermo Fisher Scientific). These served as a proxy for ^{18}O enrichment of soil water over time. We used them to calculate the average ^{18}O enrichment over the course of incubation by fitting a negative exponential function and determining its integral according to Canarini *et al.* (*69*). Our samples approached the target enrichment (70 at % ^{18}O) after 48 hours (fig. S12) but did not fully reach it. Hence, the average soil water enrichment over the 5-day incubations was 32 to 37 at % per sample.

After incubation, soil aliquots were flash-frozen and stored at −80°C. Following manufacturer's instructions, we isolated DNA from soils using the FastDNA SPIN Kit for Soil (MP Biomedicals). DNA concentrations were quantified fluorometrically using the PicoGreen Assay (Quant-iTTM PicoGreen dsDNA Reagent, Life Technologies) on a TECAN Infinite 200 PRO plate reader. To determine at % excess ^{18}O (APE ^{18}O) of our DNA extracts, we analyzed their ^{18}O isotopic composition on a thermochemical elemental analyzer (TC/EA, Thermo Fisher Scientific) coupled via a Conflo III open split system (Thermo Fisher Scientific) to an IRMS (Delta V Advantage, Thermo Fisher Scientific). DNA extracts were separated on the basis of their density to detect underlying patterns in ^{18}O isotope incorporation by ultracentrifugation in a cesium chloride density gradient (*28*). We loaded 2 µg of DNA into a 4.7-ml OptiSeal ultracentrifuge tube (Beckman Coulter) with ~4 ml of saturated CsCl solution and gradient buffer (100 mM tris, 100 mM KCl, and 1 mM EDTA). Two replicates from the root-exclusion core experiment incubated at elevated temperatures showed lower DNA yields. Hence, only 750 ng of DNA could be loaded into the ultracentrifuge tubes. For comparability reasons and downstream calculations, this was considered by multiplying DNA and 16*S* rRNA gene copies by a correction factor of 2.67. DNA samples were spun in a Beckman Optima ultracentrifuge using a Beckman VTi 90 rotor (50,000 rpm at 20°C) for 72 hours. We manually collected 24 fractions of 250 µl after puncturing the tubes with a cannula (Braun Sterican, 0.9 mm by 25 mm), while mineral oil served as a displacement medium. During fractionation, tubes were secured with a three-prong clamp attached to a retort stand. We measured the density of each fraction with a Krüss DR301-95 digital refractometer. DNA was purified from the CsCl solution by glycogen-aided isopropanol precipitation, resuspended in 50 µl of nuclease-free water, and quantified by PicoGreen fluorescence (see above).

Sequencing was performed (15 to 16 fractions per sample) at the Joint Microbiome Facility of the Medical University of Vienna and the University of Vienna (JMF project ID: JMF-2107-05). Fractions were selected on the basis of DNA content excluding those without detectable DNA. A two-step barcoding approach was used to generate amplicon libraries of archaeal and bacterial communities using Illumina MiSeq (V3 Kit) in the 2× 300–base pair configuration (*70*). Primer sequences (515F-806R) and polymerase chain reaction (PCR) amplification protocols (30 cycles) were used as specified by the Earth Microbiome Project (*71*) standard protocols (https://earthmicrobiome.org/protocols-and-standards/16s/). We used the following cycling conditions: initial denaturation at 94°C for 4 min, seven cycles of 94°C for 30 s, 52°C for 30 s, 72°C for 60 s, and final elongation at 72°C for 7 min (*70*). Amplicon pools were extracted from the raw sequencing data using the FASTQ workflow in BaseSpace (Illumina) with default parameters. Demultiplexing was performed with the python package demultiplex (Laros JFJ, github.com/jfjlaros/demultiplex) allowing one mismatch for barcodes and two mismatches for linkers and primers (*70*). ASVs were inferred using the DADA2 R package (*72*) applying the recommended workflow. FASTQ reads 1 and 2 were trimmed at 220 and 150 nt with allowed expected errors of 2 and 2, respectively. ASV sequences were subsequently classified using DADA2 and the SILVA database SSU Ref NR 99 release 138.1 (*73*, *74*) using a confidence threshold of 0.5. Datasets were deposited in the National Center for Biotechnology Information (NCBI) Sequence Read Archive under BioProject accession number PRJNA1013152.

We measured the concentration of total 16*S* rRNA gene copies per fraction on the Bio-Rad QX200 digital droplet PCR (ddPCR) system using the same primers used for sequencing but without adapters. Individual PCR reactions comprised the following components: 11 µl of 1× EvaGreen Droplet Generation Mix (Bio-Rad), 0.2 µl of forward primer (10 µM), 0.2 µl of reverse primer (10 µM), 8.6 µl of nuclease-free water, and 2 µl of diluted DNA template. Before ddPCR quantification, DNA samples were diluted to 0.05 ng/µl as 0.1 ng of total DNA per reaction was found optimal for the separation of negative and positive droplets. The following cycling conditions were used for ddPCR: 95°C for 5 min, five cycles of 95°C for 30 s, 57°C for 2.5 min (−1°C each step), followed by 35 cycles of 95°C for 30 s, 52°C for 2.5 min, followed by 4°C for 5 min, and 90°C for 5 min. Droplets were stored at 4°C for a least 1 hour before reading. We used QuantaSoft software (Bio-Rad) to calculate 16*S* rRNA gene copies.

Downloaded from https://www.science.org on June 23, 2025

Microbial community growth

We used the ^{18}O enrichment of our DNA samples before ultracentrifugation together with the estimates of microbial biomass carbon (C_{mic}) and the DNA content to calculate microbial community growth, including other microorganisms such as fungi, as described before (*8*, *20*, *75*). In short, we determined DNA production ($DNA_{produced}$) using the difference in ^{18}O abundance between labeled and natural abundance samples using a factor of 31.21 [proportional mass of O (%) in an average DNA molecule]. Microbial community growth (G, expressed as μg carbon per hour per gram of dry soil) was then calculated by multiplying DNA production with the quotient of microbial biomass carbon and DNA content [$G = DNA_{produced} * (C_{mic}/\text{Total DNA})$]. We determined microbial community growth per unit of microbial biomass (G_m, relative community growth or mass-specific growth, expressed as micrograms of carbon per hour per gram of microbial biomass carbon) using $G_m = G/C_{mic}$.

qSIP and statistical analyses

All analyses were performed in R 4.1.1 (*76*). Amplicon sequencing data was manipulated using the phyloseq package (*77*). We removed ASVs without taxonomic assignment at the phylum level or classified eukaryotes, mitochondria, or chloroplasts (2553 ASVs). In addition, we removed contaminant ASVs identified by decontam 1.6.0 (*78*) using the prevalence method and a threshold setting of 0.01. Negative controls from DNA extraction and dilution steps served as input data (number of negative controls = 6). Only samples with >2000 reads were retained for further analyses. After filtering, we yielded a feature table with 19,092 ASVs and 10,139,236 reads.

We determined weighted average densities (WADs) at the sample level, as explained by Hungate *et al.* (*28*). Previous reports suggest that variations in CsCl gradients between independent ultracentrifugation runs affect WAD estimates (*54*, *79*). Thus, we used direct IRMS measurements of the ^{18}O composition of our unfractionated DNA to calibrate WADs as described by Papp *et al.* (*80*). The calibration was based on a previously described (*28*) relationship between density and $APE^{18}O$ of DNA: expected WAD = 0.0644 * $APE^{18}O$ of DNA + 1.6946. The intercept represents the density of *Escherichia coli* DNA at natural abundance. Because density measurements can vary considerably between labs, we replaced this term with the density estimates of our unlabeled control samples. A correction factor was determined by subtracting the measured WADs from the expected WADs and then applied to the measured WADs. One sample pair (control, labeled) from the root-ingrowth treatment at ambient temperatures was spun in a slightly less concentrated CsCl gradient, resulting in overall lower WADs. To account for this, we calculated the mean offset in WAD from the control samples of the remaining replicates of the same treatment and added it to the density estimates.

Taxon-specific ^{18}O enrichment (APE ^{18}O), a proxy for microbial growth, was determined on the basis of the relationships between ^{18}O incorporation, DNA density, Guanin, Cytosin (GC) content, and DNA molecular weight as described in Hungate *et al.* (*28*). We used publicly available code to perform qSIP calculations [https://bitbucket.org/QuantitativeSIP/qsip_repo, https://github.com/bramstone/qsip, and https://doi.org/10.5281/zenodo.8109566; (*29*)]. A presence-absence filtering step was applied before qSIP analysis to exclude infrequent taxa (*14*). Taxa had to occur in at least four fractions and two replicates per treatment, yielding 7601 ASVs and accounting for 85% of all sequence reads. We calculated taxon-specific APE ^{18}O values, first, at the treatment level by bootstrap resampling of replicates and, second, at the replicate level without bootstrap resampling. Bootstrap testing allowed us to estimate whether taxon-specific density shifts via ^{18}O incorporation were consistent across replicates, resulting in a single enrichment value (bootstrap mean or median) for each taxon (*28*). To also harness growth variations between replicates, we merged both approaches by first identifying consistently growing taxa at the treatment level using bootstrap resampling and then determining their individual growth rates at the replicate level. Hence, we considered a taxon to be actively growing if its bootstrapped and non-bootstrapped APE ^{18}O values were > 0. Taxon-level RGRs per day were calculated as follows assuming linear growth: RGR = AFE $^{18}O_{taxon}$/(Average AFE $^{18}O_{soil\ water}$ * days of incubation) (*48*, *81*). For this, APE ^{18}O percent values were converted into decimals also called ^{18}O atom fraction excess (AFE ^{18}O) and commonly used in qSIP studies.

Absolute abundances (16*S* rRNA gene copies per ASV per g of dry soil) were calculated for each ASV individually by multiplying their sequencing-inferred relative abundances by the total amount of 16*S* rRNA gene copies of each fraction before summing over all fractions of a sample. To determine the size, or percentage, of the actively growing community, we summed the absolute abundances of all growing taxa and divided it by the sum of the absolute abundances of all taxa. Before summing the absolute abundances of the growing taxa, we multiplied them by their AFE ^{18}O values. By doing so, we aimed to estimate how many 16*S* rRNA gene copies were labeled within the population of a growing taxon (= size of growing subpopulation). We accounted for this because qSIP targets populations and not cells, and it is possible that only a subfraction of a taxon's population was growing. By multiplying the absolute abundance of a growing taxon by its AFE ^{18}O, we assumed that the enrichment of a taxon represents its abundance of fully labeled 16*S* rRNA gene copies. Although this is a conservative approach because there are probably also partially labeled 16*S* rRNA gene copies, it avoids overestimating the size of the growing community.

Because microbial community growth estimates (G and G_m), as described above, inherently included other microorganisms such as fungi, we additionally calculated the total rates and RGRs of the bacterial community. Total bacterial growth, expressed as the amount of produced 16*S* rRNA gene copies per gram of dry soil per day, was determined by summing the total growth across all growing taxa per day ($\sum RGR_{ASV}$ * 16*S* rRNA gene copies per gram dry $soil_{ASV}$) (*49*). Relative bacterial community growth was then calculated by dividing total growth by the size of the total bacterial community (16*S* rRNA gene copies per gram of dry soil).

We compared the effects of long-term warming on carbon and nitrogen pools (total and microbial), 16*S* rRNA gene copies, and soil moisture using two-sided Student's *t* tests when testing for overarching effects or two-way ANOVA (factors: $Warming_{ambient/+6°C}$ and $Core_{undisturbed/root\ ingrowth/root\ exclusion}$). When parametric testing was performed, we examined whether normality (Shapiro-Wilk test) and homoscedasticity (Levene's test) requirements were fulfilled and applied log transformation if necessary. To focus on the impact of root presence on extracellular enzyme activities including its interaction with warming, we used two-way ANOVA but excluded the undisturbed cores.

To assess community shifts of the total and active community (subset based on growth), we computed Euclidean distances based on ASV absolute abundances followed by two-way PERMANOVA tests with the "adonis" function (*82*). Absolute abundances were summed

Downloaded from https://www.science.org on June 23, 2025

over all fractions per sample (only labeled) and, according to a recently introduced quantitative sequencing framework (*83*), centered log-transformed before performing a PCA.

We compared RGRs, ASV richness, total bacterial growth, relative bacterial community growth, and active population sizes across treatments using two-way ANOVA (factors: $Warming_{ambient/+6°C}$ and $Core_{undisturbed/root\ ingrowth/root\ exclusion}$) followed by Tukey post hoc tests. To avoid pseudo-replication (multiple taxon-specific growth estimates per sample), we calculated mean RGRs for each sample before testing. For pairwise comparisons of RGRs of taxa shared between warming levels, we used two-sided Student's *t* tests. In addition, we used three-way ANOVA (factors: $Warming_{ambient/+6°C}$, $Core_{root\ ingrowth/root\ exclusion}$, and $Experiment_{undisturbed\ cores,in\ situ\ cores}$) to compare mean RGRs of taxa that were active in either distinct or multiple treatments (exclusive shared) to infer whether taxa associated with warming or root presence show different response levels.

We calculated how the number of growing taxa within major phyla and families shifted with long-term warming in the undisturbed cores as an indicator of their taxonomic response. We tested for significant shifts using separate nonparametric Kruskal-Wallis rank sum tests and corrected for multiple comparisons using false detection rate. Shifts in the number of growing taxa were visualized across families and phyla using relative changes between ambient and warmed conditions (0 = no change and 1 = increase by 100%). Relative changes were calculated using the following equation: (Growing ASV $richness_{Warmed}$/Mean growing ASV $richness_{Ambient}$) −1.

Although some taxa might be growing faster than others, their contribution to the overall community-level growth will also depend on their abundance. Therefore, we estimated proportional ^{18}O assimilation, or proportion of growth, for each growing ASV by recalculating their relative abundances (sum of relative abundances of growing taxa = 1) and multiplying them by their RGR. These weighted enrichment values were then divided by their sum, producing a proportional ^{18}O assimilation value ranging between 0 and 1. We ranked ASVs that were growing in at least two replicates on the basis of their proportional ^{18}O assimilation to identify the top 15 ^{18}O-assimilating taxa per sample, the top 15 ^{18}O-assimilating families per treatment, and how many taxa accounted for 50% of the total community's growth. We visualized changes in proportional ^{18}O assimilation with heatmaps using functions from the ampvis2 package (*84*). To test for significant differences in proportional ^{18}O assimilation between warming levels or root-ingrowth and root-exclusion cores at the family level, we used pairwise Wilcoxon signed-rank tests using false detection rate correction for multiple comparisons.

Supplementary Materials

This PDF file includes:
Tables S1 and S2
Figs. S1 to S12
Legends for data files S1 to S4

Other Supplementary Material for this manuscript includes the following:
Data files S1 to S4

REFERENCES AND NOTES

1. R. Cavicchioli, W. J. Ripple, K. N. Timmis, F. Azam, L. R. Bakken, M. Baylis, M. J. Behrenfeld, A. Boetius, P. W. Boyd, A. T. Classen, T. W. Crowther, R. Danovaro, C. M. Foreman, J. Huisman, D. A. Hutchins, J. K. Jansson, D. M. Karl, B. Koskella, D. B. M. Welch, J. B. H. Martiny, M. A. Moran, V. J. Orphan, D. S. Reay, J. V. Remais, V. I. Rich, B. K. Singh, L. Y. Stein, F. J. Stewart, M. B. Sullivan, M. J. H. van Oppen, S. C. Weaver, E. A. Webb, N. S. Webster, Scientists' warning to humanity: Microorganisms and climate change. *Nat. Rev. Microbiol.* **17**, 569–586 (2019).
2. D. A. Hutchins, J. K. Jansson, J. V. Remais, V. I. Rich, B. K. Singh, P. Trivedi, Climate change microbiology—problems and perspectives. *Nat. Rev. Microbiol.* **17**, 391–396 (2019).
3. W. R. Wieder, G. B. Bonan, S. D. Allison, Global soil carbon projections are improved by modelling microbial processes. *Nat. Clim. Chang.* **3**, 909–912 (2013).
4. J. W. Raich, C. S. Potter, Global patterns of carbon dioxide emissions from soils. *Global Biogeochem. Cycles* **9**, 23–36 (1995).
5. T. W. Crowther, S. M. Thomas, D. S. Maynard, P. Baldrian, K. Covey, S. D. Frey, L. T. A. van Diepen, M. A. Bradford, Biotic interactions mediate soil microbial feedbacks to climate change. *Proc. Natl. Acad. Sci. U.S.A.* **112**, 7033–7038 (2015).
6. K. Karhu, M. D. Auffret, J. A. J. Dungait, D. W. Hopkins, J. I. Prosser, B. K. Singh, J.-A. Subke, P. A. Wookey, G. I. Ågren, M.-T. Sebastià, F. Gouriveau, G. Bergkvist, P. Meir, A. T. Nottingham, N. Salinas, I. P. Hartley, Temperature sensitivity of soil respiration rates enhanced by microbial community response. *Nature* **513**, 81–84 (2014).
7. M. A. Bradford, R. L. McCulley, T. W. Crowther, E. E. Oldfield, S. A. Wood, N. Fierer, Cross-biome patterns in soil microbial respiration predictable from evolutionary theory on thermal adaptation. *Nat. Ecol. Evol.* **3**, 223–231 (2019).
8. T. W. N. Walker, C. Kaiser, F. Strasser, C. W. Herbold, N. I. W. Leblans, D. Woebken, I. A. Janssens, B. D. Sigurdsson, A. Richter, Microbial temperature sensitivity and biomass change explain soil carbon loss with warming. *Nat. Clim. Chang.* **8**, 885–889 (2018).
9. L. A. Domeignoz-Horta, G. Pold, H. Erb, D. Sebag, E. Verrecchia, T. Northen, K. Louie, E. Eloe-Fadrosh, C. Pennacchio, M. A. Knorr, S. D. Frey, J. M. Melillo, K. M. DeAngelis, Substrate availability and not thermal-acclimation controls microbial temperature sensitivity response to long term warming. *Glob. Chang. Biol.* **29**, 1574–1590 (2022).
10. J. K. Jansson, K. S. Hofmockel, Soil microbiomes and climate change. *Nat. Rev. Microbiol.* **18**, 35–46 (2020).
11. D. Naylor, N. Sadler, A. Bhattacharjee, E. B. Graham, C. R. Anderton, R. McClure, M. Lipton, K. S. Hofmockel, J. K. Jansson, Soil microbiomes under climate change and implications for carbon cycling. *Annu. Rev. Env. Resour.* **45**, 29–59 (2020).
12. A. T. Classen, M. K. Sundqvist, J. A. Henning, G. S. Newman, J. A. M. Moore, M. A. Cregger, L. C. Moorhead, C. M. Patterson, Direct and indirect effects of climate change on soil microbial and soil microbial-plant interactions: What lies ahead? *Ecosphere* **6**, art130 (2015).
13. P. Trivedi, B. D. Batista, K. E. Bazany, B. K. Singh, Plant–microbiome interactions under a changing world: Responses, consequences and perspectives. *New Phytol.* **234**, 1951–1959 (2022).
14. B. W. Stone, J. Li, B. J. Koch, S. J. Blazewicz, P. Dijkstra, M. Hayer, K. S. Hofmockel, X.-J. A. Liu, R. L. Mau, E. M. Morrissey, Nutrients cause consolidation of soil carbon flux to small proportion of bacterial community. *Nat. Commun.* **12**, 3381 (2021).
15. S. D. Allison, M. D. Wallenstein, M. A. Bradford, Soil-carbon response to warming dependent on microbial physiology. *Nat. Geosci.* **3**, 336–340 (2010).
16. C. Neill, J. Gignoux, Soil organic matter decomposition driven by microbial growth: A simple model for a complex network of interactions. *Soil Biol. Biochem.* **38**, 803–811 (2006).
17. E. Blagodatskaya, Y. Kuzyakov, Active microorganisms in soil: Critical review of estimation criteria and approaches. *Soil Biol. Biochem.* **67**, 192–211 (2013).
18. J. K. Jansson, K. S. Hofmockel, The soil microbiome—From metagenomics to metaphenomics. *Curr. Opin. Microbiol.* **43**, 162–168 (2018).
19. P. Dijkstra, A. Martinez, S. C. Thomas, C. O. Seymour, W. Wu, M. A. Dippold, J. P. Megonigal, E. Schwartz, B. A. Hungate, On maintenance and metabolisms in soil microbial communities. *Plant and Soil* **476**, 385–396 (2022).
20. E. Simon, A. Canarini, V. Martin, J. Séneca, T. Böckle, D. Reinthaler, E. M. Pötsch, H.-P. Piepho, M. Bahn, W. Wanek, Microbial growth and carbon use efficiency show seasonal responses in a multifactorial climate change experiment. *Commun. biol.* **3**, 584 (2020).
21. X. J. A. Liu, G. Pold, L. A. Domeignoz-Horta, K. M. Geyer, H. Caris, H. Nicolson, K. M. Kemner, S. D. Frey, J. M. Melillo, K. M. DeAngelis, Soil aggregate-mediated microbial responses to long-term warming. *Soil Biol. Biochem.* **152**, 108055 (2021).
22. M. A. Bradford, C. A. Davies, S. D. Frey, T. R. Maddox, J. M. Melillo, J. E. Mohan, J. F. Reynolds, K. K. Treseder, M. D. Wallenstein, Thermal adaptation of soil microbial respiration to elevated temperature. *Ecol. Lett.* **11**, 1316–1327 (2008).
23. A. L. Romero-Olivares, S. D. Allison, K. K. Treseder, Soil microbes and their response to experimental warming over time: A meta-analysis of field studies. *Soil Biol. Biochem.* **107**, 32–40 (2017).
24. N. Fanin, M. Mooshammer, M. Sauvadet, C. Meng, G. Alvarez, L. Bernard, I. Bertrand, E. Blagodatskaya, L. Bon, S. Fontaine, S. Niu, G. Lashermes, T. L. Maxwell, M. N. Weintraub, L. Wingate, D. Moorhead, A. T. Nottingham, Soil enzymes in response to climate warming: Mechanisms and feedbacks. *Funct. Ecol.* **36**, 1378–1395 (2022).
25. A. Söllinger, J. Séneca, M. Borg Dahl, L. L. Motleleng, J. Prommer, E. Verbruggen, B. D. Sigurdsson, I. Janssens, J. Peñuelas, T. Urich, A. Richter, A. T. Tveit, Down-regulation of the bacterial protein biosynthesis machinery in response to weeks, years, and decades of soil *warming*. *Sci. Adv.* **8**, eabm3230 (2022).

Downloaded from https://www.science.org on June 23, 2025

26. S. Marañón-Jiménez, J. L. Soong, N. I. W. Leblans, B. D. Sigurdsson, J. Peñuelas, A. Richter, D. Asensio, E. Fransen, I. A. Janssens, Geothermally warmed soils reveal persistent increases in the respiratory costs of soil microbes contributing to substantial C losses. *Biogeochemistry* **138**, 245–260 (2018).
27. N. Fierer, M. A. Bradford, R. B. Jackson, Toward an ecological classification of soil bacteria. *Ecology* **88**, 1354–1364 (2007).
28. B. A. Hungate, R. L. Mau, E. Schwartz, J. Gregory Caporaso, P. Dijkstra, N. van Gestel, B. J. Koch, C. M. Liu, T. A. McHugh, J. C. Marks, E. M. Morrissey, L. B. Price, Quantitative microbial ecology through stable isotope probing. *Appl. Environ. Microbiol.* **81**, 7570–7581 (2015).
29. D. Metze, J. Schnecker, A. Canarini, L. Fuchslueger, B. J. Koch, B. W. Stone, B. A. Hungate, B. Hausmann, H. Schmidt, A. Schaumberger, M. Bahn, C. Kaiser, A. Richter, Microbial growth under drought is confined to distinct taxa and modified by potential future climate conditions. *Nat. Commun.* **14**, 5895 (2023).
30. K. Fan, H. Holland-Moritz, C. Walsh, X. Guo, D. Wang, Y. Bai, Y. Zhu, N. Fierer, H. Chu, Identification of the rhizosphere microbes that actively consume plant-derived carbon. *Soil Biol. Biochem.* **166**, 108577 (2022).
31. J. L. López, A. Fourie, S. W. M. Poppeliers, N. Pappas, J. J. Sánchez-Gil, R. de Jonge, B. E. Dutilh, Growth rate is a dominant factor predicting the rhizosphere effect. *ISME J.* **17**, 1396–1405 (2023).
32. R. D. Bardgett, P. Manning, E. Morriën, F. T. De Vries, Hierarchical responses of plant–soil interactions to climate change: Consequences for the global carbon cycle. *J. Ecol.* **101**, 334–343 (2013).
33. F. I. Pugnaire, J. A. Morillo, J. Peñuelas, P. B. Reich, R. D. Bardgett, A. Gaxiola, D. A. Wardle, W. H. van der Putten, Climate change effects on plant-soil feedbacks and consequences for biodiversity and functioning of terrestrial ecosystems. *Sci. Adv.* **5**, eaaz1834 (2023).
34. R. D. Bardgett, C. Freeman, N. J. Ostle, Microbial contributions to climate change through carbon cycle feedbacks. *ISME J.* **2**, 805–814 (2008).
35. A. Malhotra, D. J. Brice, J. Childs, J. D. Graham, E. A. Hobbie, H. Vander Stel, S. C. Feron, P. J. Hanson, C. M. Iversen, Peatland warming strongly increases fine-root growth. *Proc. Natl. Acad. Sci. U.S.A.* **117**, 17627–17634 (2020).
36. S. Kwatcho Kengdo, D. Peršoh, A. Schindlbacher, J. Heinzle, Y. Tian, W. Wanek, W. Borken, Long-term soil warming alters fine root dynamics and morphology, and their ectomycorrhizal fungal community in a temperate forest soil. *Glob. Chang. Biol.* **28**, 3441–3458 (2022).
37. C. Fang, N. Verbrigghe, B. D. Sigurdsson, I. Ostonen, N. I. W. Leblans, S. Marañón-Jiménez, L. Fuchslueger, P. Sigurðsson, K. Meeran, M. Portillo-Estrada, E. Verbruggen, A. Richter, J. Sardans, J. Peñuelas, M. Bahn, S. Vicca, I. A. Janssens, Decadal soil warming decreased vascular plant above and belowground production in a subarctic grassland by inducing nitrogen limitation. *New Phytol.* **240**, 565–576 (2023).
38. B. Bhattarai, B. D. Sigurdsson, P. Sigurdsson, N. Leblans, I. Janssens, W. Meynzer, A. K. Devarajan, J. Truu, M. Truu, I. Ostonen, Soil warming duration and magnitude affect the dynamics of fine roots and rhizomes and associated C and N pools in subarctic grasslands. *Ann. Bot.* **132**, 269–279 (2023).
39. C. Wang, E. M. Morrissey, R. L. Mau, M. Hayer, J. Piñeiro, M. C. Mack, J. C. Marks, S. L. Bell, S. N. Miller, E. Schwartz, P. Dijkstra, B. J. Koch, B. W. Stone, A. M. Purcell, S. J. Blazewicz, K. S. Hofmockel, J. Pett-Ridge, B. A. Hungate, The temperature sensitivity of soil: Microbial biodiversity, growth, and carbon mineralization. *ISME J.* **15**, 2738–2747 (2021).
40. A. A. Malik, J. Puissant, T. Goodall, S. D. Allison, R. I. Griffiths, Soil microbial communities with greater investment in resource acquisition have lower growth yield. *Soil Biol. Biochem.* **132**, 36–39 (2019).
41. A. A. Malik, J. B. H. Martiny, E. L. Brodie, A. C. Martiny, K. K. Treseder, S. D. Allison, Defining trait-based microbial strategies with consequences for soil carbon cycling under climate change. *ISME J.* **14**, 1–9 (2020).
42. C. S. Sheik, W. H. Beasley, M. S. Elshahed, X. Zhou, Y. Luo, L. R. Krumholz, Effect of warming and drought on grassland microbial communities. *ISME J.* **5**, 1692–1700 (2011).
43. J. D. Rocca, M. Simonin, J. R. Blaszczak, J. G. Ernakovich, S. M. Gibbons, F. S. Midani, A. D. Washburne, The microbiome stress project: Toward a global meta-analysis of environmental stressors and their effects on microbial communities. *Front. Microbiol.* **9**, 3272 (2019).
44. A. A. Carrell, M. Kolton, J. B. Glass, D. A. Pelletier, M. J. Warren, J. E. Kostka, C. M. Iversen, P. J. Hanson, D. J. Weston, Experimental warming alters the community composition, diversity, and N_2 fixation activity of peat moss (*Sphagnum fallax*) microbiomes. *Glob. Chang. Biol.* **25**, 2993–3004 (2019).
45. J. R. Propster, E. Schwartz, M. Hayer, S. Miller, V. Monsaint-Queeney, B. J. Koch, E. M. Morrissey, M. C. Mack, B. A. Hungate, Distinct growth responses of tundra soil bacteria to short-term and long-term warming. *Appl. Environ. Microbiol.* **89**, e01543–e01522 (2023).
46. R. Rijkers, M. Dekker, R. Aerts, J. T. Weedon, Maximum summer temperatures predict the temperature adaptation of Arctic soil bacterial communities. *Biogeosciences* **20**, 767–780 (2023).
47. D. Tilman, "Some thoughts on resource competition and diversity in plant communities" in *Mediterranean-Type Ecosystems*, F. J. Kruger, D. T. Mitchell, J. U. M. Jarvis, Eds. (Springer Berlin Heidelberg, 1983), pp. 322–336.
48. A. M. Purcell, M. Hayer, B. J. Koch, R. L. Mau, S. J. Blazewicz, P. Dijkstra, M. C. Mack, J. C. Marks, E. M. Morrissey, J. Pett-Ridge, R. L. Rubin, E. Schwartz, N. C. van Gestel, B. A. Hungate, Decreased growth of wild soil microbes after 15 years of transplant-induced warming in a montane meadow. *Glob. Chang. Biol.* **28**, 128–139 (2021).
49. A. M. Purcell, P. Dijkstra, B. A. Hungate, K. McMillen, E. Schwartz, N. van Gestel, Rapid growth rate responses of terrestrial bacteria to field warming on the Antarctic Peninsula. *ISME J.* **17**, 2290–2302 (2023).
50. L. Zhou, X. Zhou, Y. He, Y. Fu, Z. Du, M. Lu, X. Sun, C. Li, C. Lu, R. Liu, G. Zhou, S. H. Bai, M. P. Thakur, Global systematic review with meta-analysis shows that warming effects on terrestrial plant biomass allocation are influenced by precipitation and mycorrhizal association. *Nat. Commun.* **13**, 4914 (2022).
51. M. Liu, J.-H. Wen, Y.-M. Chen, W.-J. Xu, Q. Wang, Z.-L. Ma, Warming increases soil carbon input in a Sibiraea angustata-dominated alpine shrub ecosystem. *J. Plant Ecol.* **15**, 335–346 (2022).
52. F. M. Hopkins, T. R. Filley, G. Gleixner, M. Lange, S. M. Top, S. E. Trumbore, Increased belowground carbon inputs and warming promote loss of soil organic carbon through complementary microbial responses. *Soil Biol. Biochem.* **76**, 57–69 (2014).
53. Y. Qiu, L. Guo, X. Xu, L. Zhang, K. Zhang, M. Chen, Y. Zhao, K. O. Burkey, H. D. Shew, R. W. Zobel, Y. Zhang, S. Hu, Warming and elevated ozone induce tradeoffs between fine roots and mycorrhizal fungi and stimulate organic carbon decomposition. *Sci. Adv.* **7**, eabe9256 (2021).
54. E. M. Morrissey, R. L. Mau, M. Hayer, X.-J. A. Liu, E. Schwartz, P. Dijkstra, B. J. Koch, K. Allen, S. J. Blazewicz, K. Hofmockel, J. Pett-Ridge, B. A. Hungate, Evolutionary history constrains microbial traits across environmental variation. *Nat. Ecol. Evol.* **3**, 1064–1069 (2019).
55. B. R. K. Roller, T. M. Schmidt, The physiology and ecological implications of efficient growth. *ISME J.* **9**, 1481–1487 (2015).
56. C. Song, R. Schmidt, V. de Jager, D. Krzyzanowska, E. Jongedijk, K. Cankar, J. Beekwilder, A. van Veen, W. de Boer, J. A. van Veen, P. Garbeva, Exploring the genomic traits of fungus-feeding bacterial genus *Collimonas*. *BMC Genomics* **16**, 1103 (2015).
57. Y. Takahashi, Genus *Kitasatospora*, taxonomic features and diversity of secondary metabolites. *J. Antibiot.* **70**, 506–513 (2017).
58. A. Malik, Y. R. Kim, S. B. Kim, Genome mining of the genus *Streptacidiphilus* for biosynthetic and biodegradation potential. *Genes. (Basel)* **11**, 1166 (2020).
59. J. E. Pérez-Jaramillo, V. J. Carrión, M. Bosse, L. F. V. Ferrão, M. de Hollander, A. A. F. Garcia, C. A. Ramírez, R. Mendes, J. M. Raaijmakers, Linking rhizosphere microbiome composition of wild and domesticated *Phaseolus vulgaris* to genotypic and root phenotypic traits. *ISME J.* **11**, 2244–2257 (2017).
60. A. Znój, J. Gawor, R. Gromadka, K. J. Chwedorzewska, J. Grzesiak, Root-associated bacteria community characteristics of Antarctic plants: *Deschampsia antarctica* and *Colobanthus quitensis*—A comparison. *Microb. Ecol.* **84**, 808–820 (2022).
61. J. E. Pérez-Jaramillo, V. J. Carrión, M. de Hollander, J. M. Raaijmakers, The wild side of plant microbiomes. *Microbiome* **6**, 143 (2018).
62. C. Yin, S. H. Hulbert, K. L. Schroeder, O. Mavrodi, D. Mavrodi, A. Dhingra, W. F. Schillinger, T. C. Paulitz, Role of bacterial communities in the natural suppression of *Rhizoctonia solani* bare patch disease of wheat (*Triticum aestivum* L.). *Appl. Environ. Microbiol.* **79**, 7428–7438 (2013).
63. E. Chapelle, R. Mendes, P. A. H. M. Bakker, J. M. Raaijmakers, Fungal invasion of the rhizosphere microbiome. *ISME J.* **10**, 265–268 (2016).
64. V. J. Carrión, J. Perez-Jaramillo, V. Cordovez, V. Tracanna, M. de Hollander, D. Ruiz-Buck, L. W. Mendes, W. F. J. van Ijcken, R. Gomez-Exposito, S. S. Elsayed, P. Mohanraju, A. Arifah, J. van der Oost, J. N. Paulson, R. Mendes, G. P. van Wezel, M. H. Medema, J. M. Raaijmakers, Pathogen-induced activation of disease-suppressive functions in the endophytic root microbiome. *Science* **366**, 606–612 (2019).
65. C. Dang, J. G. V. Walkup, B. A. Hungate, R. B. Franklin, E. Schwartz, E. M. Morrissey, Phylogenetic organization in the assimilation of chemically distinct substrates by soil bacteria. *Environ. Microbiol.* **24**, 357–369 (2022).
66. B. D. Sigurdsson, N. I. W. Leblans, S. Dauwe, E. Gudmundsdóttir, P. Gundersen, G. E. Gunnarsdóttir, M. Holmstrup, K. Ilieva-Makulec, T. Kätterer, B. Marteinsdóttir, M. Maljanen, E. S. Oddsdóttir, I. Ostonen, J. Peñuelas, C. Poeplau, A. Richter, P. Sigurdsson, P. Van Bodegom, H. Wallander, J. Weedon, I. Janssens, Geothermal ecosystems as natural climate change experiments: The ForHot research site in Iceland as a case study. *Icel. Agric. Sci.* **29**, 53–71 (2016).
67. E. D. Vance, P. C. Brookes, D. S. Jenkinson, An extraction method for measuring soil microbial biomass C. *Soil Biol. Biochem.* **19**, 703–707 (1987).
68. C. Kaiser, M. Koranda, B. Kitzler, L. Fuchslueger, J. Schnecker, P. Schweiger, F. Rasche, S. Zechmeister-Boltenstern, A. Sessitsch, A. Richter, Belowground carbon allocation by trees drives seasonal patterns of extracellular enzyme activities by altering microbial community composition in a beech forest soil. *New Phytol.* **187**, 843–858 (2010).

Downloaded from https://www.science.org on June 23, 2025

69. A. Canarini, W. Wanek, M. Watzka, T. Sandén, H. Spiegel, J. Šantrůček, J. Schnecker, Quantifying microbial growth and carbon use efficiency in dry soil environments via ^{18}O water vapor equilibration. *Glob. Chang. Biol.* **26**, 5333–5341 (2020).
70. P. Pjevac, B. Hausmann, J. Schwarz, G. Kohl, C. W. Herbold, A. Loy, D. Berry, An economical and flexible dual barcoding, two-step PCR approach for highly multiplexed amplicon sequencing. *Front. Microbiol.* **12**, 669776 (2021).
71. J. A. Gilbert, J. K. Jansson, R. Knight, The Earth Microbiome project: Successes and aspirations. *BMC Biol.* **12**, 69 (2014).
72. B. J. Callahan, P. J. McMurdie, M. J. Rosen, A. W. Han, A. J. A. Johnson, S. P. Holmes, DADA2: High-resolution sample inference from Illumina amplicon data. *Nat. Methods* **13**, 581–583 (2016).
73. C. Quast, E. Pruesse, P. Yilmaz, J. Gerken, T. Schweer, P. Yarza, J. Peplies, F. O. Glöckner, The SILVA ribosomal RNA gene database project: Improved data processing and web-based tools. *Nucleic Acids Res.* **41**, D590–D596 (2013).
74. M. R. McLaren, B. J. Callahan, Silva 138.1 prokaryotic SSU taxonomic training data formatted for DADA2 (2021); doi:10.5281/ZENODO.4587955.
75. M. Spohn, K. Klaus, W. Wanek, A. Richter, Microbial carbon use efficiency and biomass turnover times depending on soil depth–Implications for carbon cycling. *Soil Biol. Biochem.* **96**, 74–81 (2016).
76. R Core Team, R: A language and environment for statistical computing (R Foundation for Statistical Computing, Vienna, Austria, 2021); www.R-project.org/.
77. P. J. McMurdie, S. Holmes, phyloseq: An R package for reproducible interactive analysis and graphics of microbiome census data. *PLOS ONE* **8**, e61217 (2013).
78. N. M. Davis, D. M. Proctor, S. P. Holmes, D. A. Relman, B. J. Callahan, Simple statistical identification and removal of contaminant sequences in marker-gene and metagenomics data. *Microbiome* **6**, 226 (2018).
79. E. M. Morrissey, R. L. Mau, E. Schwartz, T. A. McHugh, P. Dijkstra, B. J. Koch, J. C. Marks, B. A. Hungate, Bacterial carbon use plasticity, phylogenetic diversity and the priming of soil organic matter. *ISME J.* **11**, 1890–1899 (2017).
80. K. Papp, B. A. Hungate, E. Schwartz, Glucose triggers strong taxon-specific responses in microbial growth and activity: Insights from DNA and RNA qSIP. *Ecology* **101**, e02887 (2020).
81. J. Li, R. L. Mau, P. Dijkstra, B. J. Koch, E. Schwartz, X.-J. A. Liu, E. M. Morrissey, S. J. Blazewicz, J. Pett-Ridge, B. W. Stone, M. Hayer, B. A. Hungate, Predictive genomic traits for bacterial growth in culture versus actual growth in soil. *ISME J.* **13**, 2162–2172 (2019).
82. J. Oksanen, F. G. Blanchet, M. Friendly, R. Kindt, P. Legendre, D. McGlinn, P. R. Minchin, R. B. O'Hara, G. L. Simpson, P. Solymos, M. H. H. Stevens, E. Szoecs, H. H. Wagner, Vegan: Community Ecology Package. R package version 2.5-6. (2019); https://CRAN.R-project.org/package=vegan.
83. J. T. Barlow, S. R. Bogatyrev, R. F. Ismagilov, A quantitative sequencing framework for absolute abundance measurements of mucosal and lumenal microbial communities. *Nat. Commun.* **11**, 2590 (2020).
84. K. S. Andersen, R. H. Kirkegaard, S. M. Karst, M. Albertsen, ampvis2: An R package to analyse and visualise 16S rRNA amplicon data. bioRxiv 10.1101/299537 (2018). https://doi.org/10.1101/299537.

Acknowledgments: We thank J. Schwarz and G. Kohl for 16*S* rRNA gene amplification and sequencing. We also thank J. Senéca Silva for handling the submission of the sequencing data to the NCBI Short Read Archive and L. Hadziabdic for optimizing the conditions for 16*S* rRNA gene amplification using ddPCR. Furthermore, we thank S. Eichorst for support with the ultracentrifuge and P. Sigurðsson for help during sampling. We also thank A. Hamedpour and Svarmi for the permission to use drone footage. **Funding:** D.M., C.L.N.d.C., and B.B. were financially supported by FutureArctic, a European Union's Horizon 2020 research and innovation program under the Marie Skłodowska-Curie Actions (grant no. 813114). **Author contributions:** D.M., A.R., C.K., E.V., and I.O. conceived the study, and B.D.S., I.A.J., and A.R. established the field site. D.M., C.L.N.d.C., and B.B. carried out fieldwork. D.M., J.S., and C.L.N.d.C. performed the lab experiments. D.M. performed data analyses. B.H. processed the raw amplicon sequencing data. D.M. and A.R. drafted the manuscript. All coauthors contributed to the revision of the manuscript. A.R., C.K., I.A.J., and B.D.S. supervised this study and together with E.V. acquired funding. **Competing interests:** The authors declare that they have no competing interests. **Data and materials availability:** All data needed to evaluate the conclusions in the paper are present in the paper and/or the Supplementary Materials. All code and data used to produce the analyses and figures of this study are openly available in the Zenodo database under accession code 10115521 (https://zenodo.org/records/10115521). DNA sequence data generated in the frame of this study have been deposited in the NCBI Short Read Archive under the BioProject accession number PRJNA1013152 (www.ncbi.nlm.nih.gov/bioproject/?term=PRJNA1013152).

Submitted 5 September 2023
Accepted 22 January 2024
Published 23 February 2024
10.1126/sciadv.adk6295

Downloaded from https://www.science.org on June 23, 2025